

Brief communication

“Modeling tornado dynamics and the generation of infrasound, electric and magnetic fields”

E. D. Schmitter

Faculty of Engineering and Computer Science, University of Applied Sciences Osnabrueck, Albrechtstr. 30, 49076 Osnabrueck, Germany

Received: 23 July 2009 – Revised: 18 January 2010 – Accepted: 9 February 2010 – Published: 16 February 2010

Abstract. Recent observations endorse earlier measurements of time varying electric and magnetic fields generated by tornadoes and dust devils. These signals may provide a means for early warning but together with a proper modeling approach can also provide insight into geometry and dynamics of the vortices. Our model calculations show the existence of pressure resonances characterized as acoustic duct modes with well defined frequencies. These resonances not only generate infrasound but also modulate the charge density and the velocity field and in this way lead to electric and magnetic field oscillations in the 0.5–20-Hz range that can be monitored from a distance of several kilometers.

1 Introduction

There is plenty of evidence that dust devils and tornadoes can be sources of infrasound as well as electric and magnetic fields slowly varying in the Hertz range, see Abdullah (1966), Bedard and Georges (2000), Bedard (2005), Schechter et al. (2008), Houser et al. (2009), Leeman and Schmitter (2009). Schechter et al. (2008) use the RAMS (Regional Atmospheric Modeling System) software environment with a model space extension up to 33 km and nested grids to study the field around a Rankine vortex generating spiral acoustic radiation. Bedard (2005) reviews observations and compares sound generation models. They suggest that their data are most consistent with the radial-modes-of-vibration model of Abdullah (1966). Our model is confined to the lower part of the vortex itself to study sources and possible generation mechanisms of sound as well as electric and magnetic fields. Significantly different results with respect to the relationship of oscillation frequency and vortex radius are obtained de-

pending on the chosen model boundary conditions. To gain some insight into the involved processes we have set up a numerical Finite Element Analysis (FEA) model that treats a vortex as a fluid dynamical system. The air-dust-water fluid carries a net charge and via its velocity distribution also yields a current density. Charges generate electric fields and current densities generate magnetic fields. Both fields are decoupled in the static limit (the involved wavelengths are extremely long with respect to the typical geometry length scales). The net charge densities used in our calculations are $\rho_c = 10^{-9} \dots 10^{-14} \text{ C/m}^3$, cp. MacGorman and Rust (1998).

2 The model

To describe the time development of the fluid velocity field \mathbf{v} and pressure p we use the compressible Navier-Stokes equation together with mass conservation:

$$\rho \left(\frac{\partial \mathbf{v}}{\partial t} + (\mathbf{v} \times \nabla) \mathbf{v} \right) = -\nabla p + \eta \left(\Delta \mathbf{v} + \frac{1}{3} \nabla (\nabla \times \mathbf{v}) \right) + \mathbf{f}$$

$$\frac{\partial \rho}{\partial t} + \nabla \times (\rho \mathbf{v}) = 0$$

where η is the dynamic viscosity. Pressure p and density ρ are related by the ideal gas law:

$$\rho(p) = \frac{M}{RT} p$$

where M is the mol mass of air, T the ambient temperature in Kelvin and R the gas constant. The volume force \mathbf{f} is the sum of gravity and the Lorentz-force:

$$\mathbf{f} = \rho \mathbf{g} + \rho_c (\mathbf{E} + \mathbf{v} \times \mathbf{B})$$

with the charge density ρ_c . The electric and magnetic field behaviour is statically approximated because of the very slowly varying sources (few Hz regime). For the electric potential Φ and the magnetic vector potential \mathbf{A} we then have



Correspondence to: E. D. Schmitter
(e.d.schmitter@fh-osnabrueck.de)

the Poisson equations (with respect to rectangular coordinates in the case of \mathbf{A}):

$$\Delta \Phi = -\frac{1}{\epsilon_0} \rho_c$$

$$\Delta A = -\mu_0 \mathbf{j}$$

with the current density $\mathbf{j} = \rho_c \mathbf{v}$.

The electric and magnetic fields then are derived from their potentials:

$$\mathbf{E} = -\nabla \Phi$$

$$\mathbf{B} = \nabla \times \mathbf{A}$$

2.1 Geometry, initial and boundary conditions

The model space is a cylinder with a radius of typically 100 m and a height of 500 m corresponding to the bottom part of a tornado. A rotating velocity field with maximum rotation velocity at half the cylinder radius (the vortex radius then is $R_v=50$ m) is given as an initial vortex condition for the fluid dynamics. A pressure field decreasing with height is also initial condition. The pressure drop is chosen to be 6% of the ambient air pressure per 500 m height. This is in accordance with measurements, cp. Hoecker (1961), Samaras and Lee (2006). It turns out that just this updraft value is needed to keep the vortex stable against gravity. Two different boundary conditions for the cylinder jacket have been used: 1. A fixed pressure boundary condition reflecting the pressure drop from bottom to top. 2. A fixed velocity ($\mathbf{v} = \mathbf{0}$) boundary condition. The velocity and pressure fields then are evolved into a valid solution of the electrically and magnetically coupled Navier-Stokes equation system in the course of the solution process. For the electric and magnetic Poisson equations a potential gradient of 100 V/m (a typical value for the lower atmosphere during undisturbed conditions) and a vanishing vector potential have been defined as initial and boundary conditions.

3 Results

Figure 1 shows a snapshot of the model space with the velocity field (top) and the electric vector field as well as the magnetic field lines (bottom) generated by the volume charge and its movement. All figures refer to the results using the fixed pressure boundary condition. Figure 2 reveals that an important part of the dynamics of the vortex is an oscillation of the pressure distribution. Shown are isobaric surfaces and the pressure gradient field (pressure volume forces) orthogonal to the surfaces. In the example case the pulsation period is 1 s and the snapshots are taken with half a second time difference. Numerical calculations of geometries with

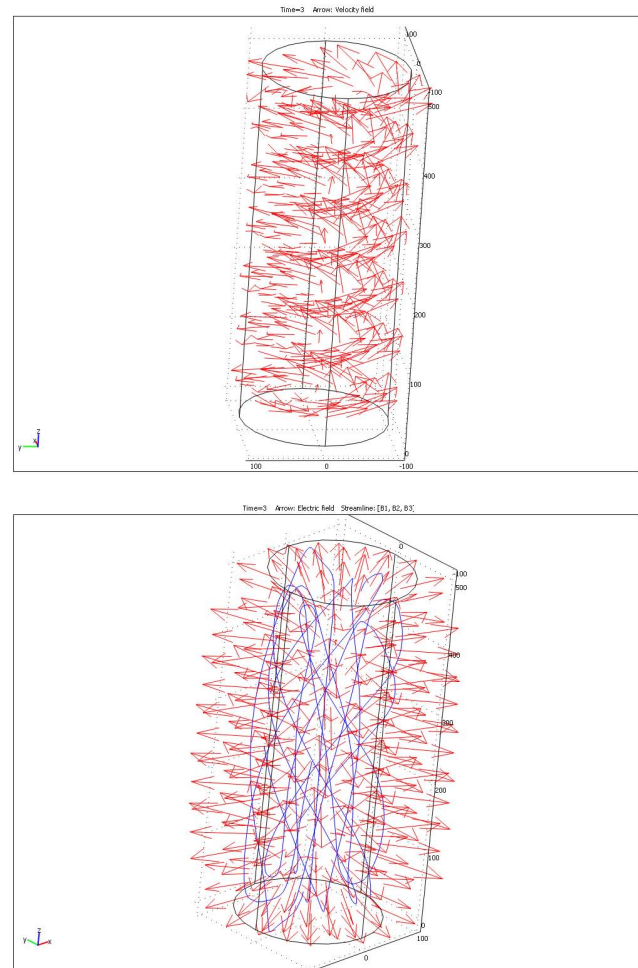


Fig. 1. Snapshot of the tornado velocity field (upper part). In the lower part: \mathbf{E} (red arrows), \mathbf{B} (blue closed lines).

different radii, heights, rotation velocities and pressure gradients balancing gravity show consistently that the frequency of the pressure pulsations or standing waves turns out to be

$$f_p \cong 2 \frac{v_{\text{sound}}}{2\pi R}$$

when the fixed pressure boundary condition is applied and

$$f_p \cong 4 \frac{v_{\text{sound}}}{2\pi R}$$

with the fixed velocity boundary condition.

$v_{\text{sound}} = 340$ m/s is the sound velocity of air, R the model radius. The latter result is in agreement with the analytically derived result by Abdullah (1966) in the limit of small maximum tangential velocity compared to v_{sound} and where also a fixed velocity boundary condition is used. The agreement with Abdullah (1966) is remarkable because it underpins our result that the detailed radial velocity profile is not important

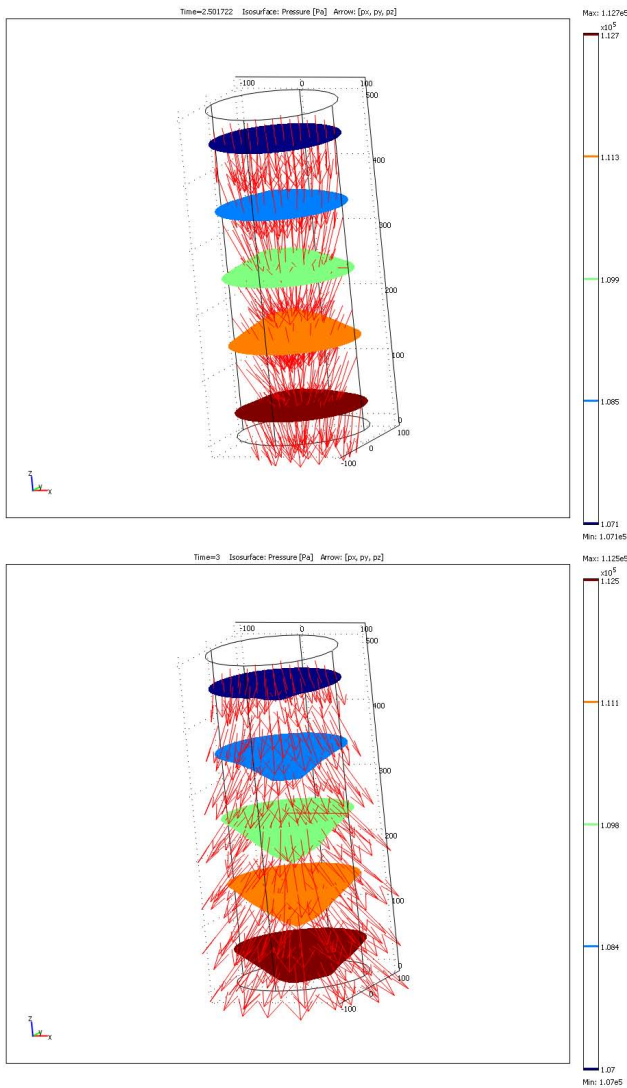


Fig. 2. Tornado pressure field oscillation – snapshots half a time period apart. Displayed are isobaric surfaces and the pressure gradient field (orthogonal to the surfaces).

for the frequency relation (he uses a flat velocity profile up to R and a $1/r$ decay beyond R whereas we use gaussian velocity profiles with varying widths and centers at $r < R$). The corresponding wavelength is equal to the circumference of the vortex in case of the fixed pressure boundary condition:

$$\lambda_p = \frac{v_{\text{sound}}}{f_p} = 2\pi R$$

and half of it in the case of a fixed velocity boundary condition. The choice of the cylinder jacket boundary condition makes a big difference and future work has to deal with their validation. We conclude that different boundary conditions prefer different modes of the well known acoustic duct waves in the limit of zero axial propagation velocity

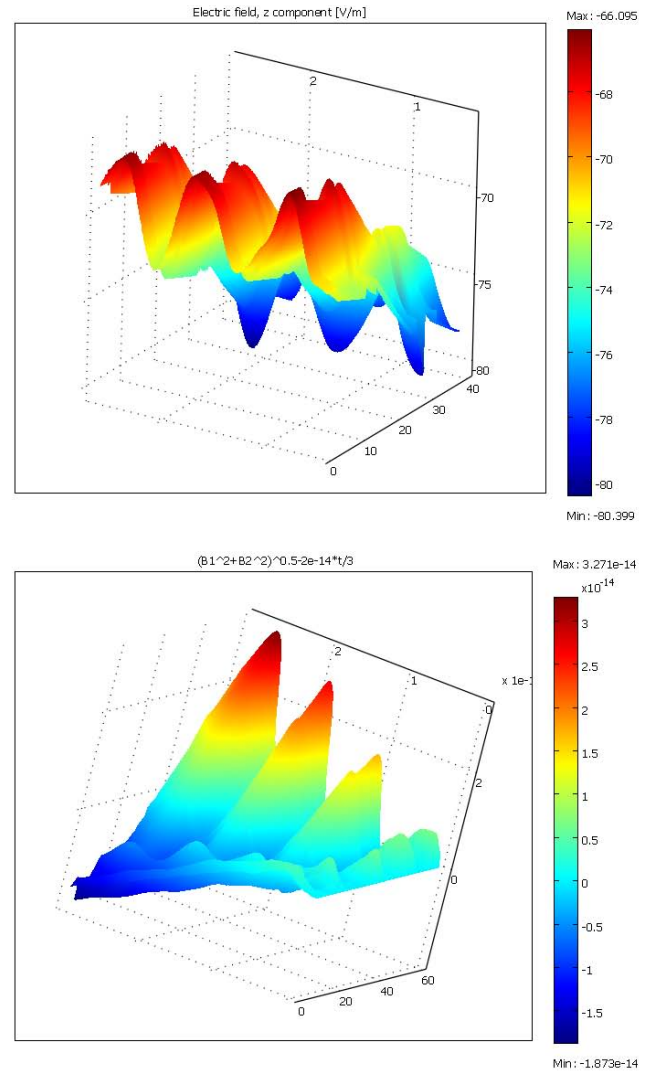


Fig. 3. Modulation of the vertical E-field component (V/m, upper part) and the horizontal B-field component (Tesla, lower part) along a radial path at half height during 3 s. Generating sources: $\rho_c=10^{-9} \text{ C/m}^3$ and max. rotation velocity $55.6 \text{ m/s}=200 \text{ km/h}$ at $R_v=50 \text{ m}$. The B-field amplitude increases because during the model run the mean updraft fluid velocity slightly picked up as a consequence of the delicate balance of pressure gradient and gravity volume force.

(standing waves or pure radial oscillations). These cut off frequencies are (Norton and Karczub, 2003)

$$f_{p,q} = \alpha_{p,q} \frac{v_{\text{sound}}}{2\pi R}$$

with $\alpha_{p,q} = 1.84$ for $p = 1, q = 0$ (triggered by a pressure boundary condition in our model) and $\alpha_{p,q} = 3.83$ for $p = 0, q = 1$ (triggered by a velocity boundary condition in our model). p is the number of plane diametral nodal surfaces and q the number of axisymmetric cylindrical nodal surfaces. For a model vortex with $R=100 \text{ m}$ this just amounts to

$f \cong 1$ Hz, $\lambda \cong 340$ m and $f \cong 2$ Hz, $\lambda \cong 170$ m for the 2 different boundary conditions. So for dust devils and tornados with a radius range of $R = 10 \dots 200$ m this amounts to a frequency range of $f = 20 \dots 0.5$ Hz. For the vortex geometry with a velocity maximum of 200 km/h at 50-m radius (corresponding to a weak F2 tornado) and 500-m height the pressure amplitude at half height is about 10^4 Pa. With a charge density of 10^{-9} C/m³ the E-field amplitude is about 10 V/m and the B-field amplitude is about 10^{-14} T. Figure 3 shows the oscillations of the vertical electric and the horizontal magnetic field components along a radial path. These are weak fields, however measurable with suitable instruments and we point out, that the E-field is directly proportional to charge density and the B-field to the product of charge density and rotation velocity. In fact E- and B-field measurements near a vortex can be used to identify mean net charge density and rotation velocity by using our model. Initialising a pressure gradient of 1.2% of ambient pressure per 100 m proves essential for maintaining the vortex. The Lorentz force term of the Navier-Stokes equations proves to be negligible compared to gravity as long as the charge density is well below 10^{-6} C/m³, cp. Dehel et al. (2007). Calculations have been done using the COMSOL[®] 3.4 software.

4 Conclusions and perspectives

Our FEA model of a vortex clearly exhibits acoustic oscillations related to the funnel diameter that modulate net charge density as a consequence of the model geometry and a delicate balance of pressure gradient and gravity volume force. Infrasound as well as electric and magnetic fields are generated. The results quantitatively explain monitored data. Using our proposed model with acoustic as well as electric and magnetic field measurement data near a tornado or dust devil allows to identify the parameters funnel diameter, rotation velocity and net charge density. Placing a few Extremely Low Frequency (ELF) receivers around or within a thunderstorm area we expect to detect vortex activity up to distances of about 10 km depending on the vortex charge density and tangential velocity. Cross-correlating data from more than one receiver allows for eliminating interfering local noise in this frequency range. Such a receiver equipment is not cost-intensive and ELF waves exhibit a much better penetration capability through high humidity volumes than high frequencies used for example by weather radars. Also the specific ELF propagation characteristics might prove electromagnetic monitoring superior to infrasound detection methods because there is no acoustic delay. Future work together with a more detailed publication is planned especially regarding the following issues: the net charge generation processes that are basic to the electromagnetic field generation, the validation of different boundary conditions of the simulation and the extension of

the model space significantly beyond the vortex. This model approach can be easily adapted to a completely different environment, for example to describe Martian dust devils.

Edited by: A. Mugnai

Reviewed by: A. Bedard and another anonymous referee

References

- Abdullah, A. J.: The musical sound of tornados, *Mon. Weather Rev.*, 94(4), 213–220, 1966.
- Bedard, A. J. and Georges, T. M.: Atmospheric infrasound, *Phys. Today*, 32–37, March 2000.
- Bedard Jr., A. J.: Low-Frequency Atmospheric Acoustic Energy Associated with Vortices Produced by Thunderstorms, *Mon. Weather Rev.*, 133, 241–263, 2005.
- Dehel, T. F., Dickinson, M., Lorge, F., and Startzel, R.: Electric field and Lorentz force contribution to atmospheric vortex phenomena, *J. Electrostat.*, 65, 631–638, 2007.
- Hoecker, W. H.: Three-dimensional pressure pattern of the Dallas tornado and some resultant implications, *Mon. Weather Rev.*, 533–542, December 1961.
- Houser, J. G., Farrell, W. M., and Metzger, S. M.: ULF and ELF magnetic activity from a terrestrial dust devil, *Geophys. Res. Lett.*, 30(1), 1027, doi:10.1029/2001GL014144, 2003.
- Leeman, J. and Schmitter, E. D.: Electric Signals Generated by Tornados, *Atmos. Res.*, 92, 277–279, 2009.
- MacGorman, D. R. and Rust, W. D.: *The electric nature of storms*, Oxford University Press, 1998.
- Norton, M. P. and Karczub, D. G.: *Fundamentals of noise and vibration analysis for engineers*, 2nd edn., Cambridge University Press, 2003.
- Samaras, T. M. and Lee, J. J.: Measuring tornado dynamics with in-situ instrumentation, *Conf. on Structural Engineering and Public Safety*, St. Louis, Missouri, USA, proceedings paper no. 4.9, 18–21 May 2006.
- Schechter, D. A., Nicholls, M. E., Persing, J., Bedard Jr., A. J., and Pielke Sr., R. A.: Infrasound Emitted by Tornado-Like Vortices: Basic Theory and a Numerical Comparison to the Acoustic Radiation of a Single-Cell Thunderstorm, *J. Atmos. Sci.*, 65, 685–713, 2008.